[CANCER RESEARCH 64, 5363–5369, August 1, 2004]

Phosphorylated Histone H2AX in Spheroids, Tumors, and Tissues of Mice Exposed to Etoposide and 3-Amino-1,2,4-Benzotriazine-1,3-Dioxide

Peggy L. Olive, Judit P. Banáth, and Laura T. Sinnott

British Columbia Cancer Research Centre, Vancouver, British Columbia, Canada

ABSTRACT

We reported recently that exposure of hamster V79 fibroblasts to 6 drugs that varied in their ability to produce DNA double-strand breaks stimulated formation of phosphorylated histone H2AX (serine 139 phosphorylated histone H2AX; γH2AX). Using flow cytometry to analyze γH2AX antibody-stained cells 1 h after a 30-min drug treatment, the fraction of cells that showed the control levels of γH2AX correlated well with the fraction of cells that survived to form colonies. This observation is now extended to V79 and SiHa human cervical carcinoma cells grown as multicell spheroids and SiHa xenografts and SCCVII tumors in mice. Animals were injected with etoposide, a topoisomerase-II inhibitor that targets proliferating cells or 3-amino-1,2,4-benzotriazine-1,3-dioxide (tirapazamine), a bioreductive cytotoxin that targets hypoxic cells. For spheroids, γH2AX intensity predicted clonogenic cell survival for cells recovered 90 min after drug injection, regardless of position of the cells within the spheroid. Similar results were obtained for etoposide in tumors; however, the γH2AX signal for tirapazamine was smaller than expected for the observed amount of cell killing. Frozen sections of tumors confirmed the greater intensity of γH2AX staining in cells close to blood vessels of tumors soon after treatment with etoposide and the opposite pattern for tumors exposed to tirapazamine. Analysis of cells or frozen sections from mouse spleen and kidney suggests that information can also be obtained on initial damage in normal tissues. These results support the possibility of using γH2AX antibody staining as a method to aid in prediction of tumor and normal tissue response to treatment.

INTRODUCTION

Chemosensitivity testing methods that measure *de novo* resistance of tumor cells are generally based on the response of cells obtained from biopsies and exposed *in vitro* to selected drugs (1). Although often successful in identifying those patients likely to respond poorly, such tests are not yet used routinely as a basis to modify treatment. Achieving that next step, truly "individualized" therapy, may require advances in several areas including a better understanding of the basis for resistance, developing treatments aimed at overcoming specific patterns of resistance, and developing techniques to rapidly measure drug response after *in situ* exposure.

DNA damage is a potential end point that might predict tumor cell survival after cytotoxins are administered *in situ*. We have used the alkaline comet assay on cells recovered from spheroids and xenograft tumors after drug treatment, and DNA damage was shown to reflect both genetic and microenvironmental resistance to selected drugs (2–4). We examined recently the ability of phosphorylated histone H2AX, an exceptionally sensitive indicator of DNA double-strand breaks, to act as a surrogate measure of lethal damage after exposure to ionizing radiation and drugs (5, 6). Induction of DNA double-strand breaks causes phosphorylation of histone H2AX at serine 139 (7), and the resulting regions covering megabases flanking each DNA double-strand break appear as spots or foci when examined microscopically after antibody staining. Those foci slowly resolve as DNA repair proceeds, yet residual foci can be observed hours to days after treatment and may represent sites of incomplete repair associated with drug/radiation sensitivity. In addition to the classic double-strand break inducing agents such as ionizing radiation, bleomycin, and neocarcinostatin, serine 139 phosphorylated histone H2AX (γH2AX) is also formed after exposure to UV, camptothecin, methylmethanesulfonate, high-dose hydrogen peroxide, doxorubicin, etoposide, and 3-amino-1,2,4-benzotriazine-1,3-dioxide (tirapazamine) (5, 8–11).

For ionizing radiation, the number of γH2AX foci correlates well with the expected number of double-strand breaks produced per Gy (12, 13). The relationship between foci number and double-strand breaks is less certain after drug treatment, where the chemical nature of the lesions, DNA replication, and the subsequent repair processes may modify the signaling pathways leading to focus formation. Despite these differences, we found that expression of γH2AX measured 1 h after a short treatment with 6 drugs could predict survival in Chinese hamster V79 monolayers (5). The fraction of cells with background γH2AX antibody staining intensity 1 h after a 30-min treatment, measured by flow cytometry, correlated with the percentage of cells that survived to form colonies (5). Moreover, predictive ability was largely independent of drug type, because γH2AX levels five times background levels resulted in 50–90% cell kill. The ability to correlate initial γH2AX levels with killing indicates that the extent of drug damage, not subsequent repair, is the critical factor for cell survival. These results also suggested that this approach might be a useful way to predict tumor cell response to treatment *in situ*. As a next step toward this goal, we have examined the relation between γH2AX formation and the cytotoxicity of etoposide and tirapazamine in more complex models of tumors–multicell spheroids and tumor xenografts growing in immunodeficient mice.

MATERIALS AND METHODS

Spheroid Culture and Treatment. SiHa human cervical carcinoma cells, from American Type Culture Collection (Manassas, VA), and V79 lung fibroblasts were maintained with twice-weekly subculture in MEM containing 10% fetal bovine serum. V79-VP^r cells were obtained in our laboratory by passage of V79 cells for 11 generations in 1 μg/ml etoposide. These cells express normal amounts of P-glycoprotein but appear to have a mutated topoisomerase-IIα protein (14). Spheroids were initiated by placing 4×10^5 SiHa cells/ml in Bellco glass spinner culture flasks (Vineland, NJ) in MEM plus 10% fetal bovine serum supplemented with antibiotics as described previously (2). Spheroids were fed daily after 3 days and used after ~2 weeks when they had reached a diameter of ~600 μm.

Spheroid Drug Treatment. Tirapazamine was obtained from Sanofi-Synthelabo Inc. and dissolved in PBS at a concentration of 2 mg/ml in PBS. Because this drug is preferentially toxic to anoxic cells, spheroids were incubated at 37°C in glass spinner culture flasks in medium equilibrated with 10% O_2, 5% CO_2, and balance N_2, a procedure that produces a hypoxic fraction of ~20% in SiHa spheroids (15). Etoposide was diluted from the 20 mg/ml stock purchased from Bristol Myers-Squibb, and spheroids were exposed under ambient oxygen conditions. For both drugs, a 30-min exposure to etoposide and tirapazamine was conducted in spinner culture flasks at 37°C. After treatment, spheroids were rinsed free of the drug and incubated for 1 h

Received 2/27/04; revised 4/28/04; accepted 5/27/04.

Grant support: Grant 12069 awarded by the National Cancer Institute of Canada with funds provided by the Canadian Cancer Society.

The costs of publication of this article were defrayed in part by the payment of page charges. This article must therefore be hereby marked *advertisement* in accordance with 18 U.S.C. Section 1734 solely to indicate this fact.

Requests for reprints: Peggy L. Olive, Medical Biophysics Department, British Columbia Cancer Research Centre, 601 West 10th Avenue, Vancouver, British Columbia V5Z 1L3, Canada. Phone: (604) 877-6000, extension 3024; Fax: (604) 877-6002; E-mail: polive@bccancer.bc.ca.

in culture flasks under ambient oxygen conditions to allow development of γH2AX foci. In some experiments, this period was extended to 48 h. For most experiments, the perfusion marker, Hoechst 33342 (1 μg/ml; Sigma) was present during the last 20 min of incubation. This fluorescent DNA binding dye provides a gradient for cell sorting that allows separation of cells from the outer and inner regions of the spheroid (16). Single cells were prepared from spheroids by a 5-min exposure to 0.25% trypsin, and cells were sorted using a Becton-Dickinson FACS 440 cell sorter into populations representing the brightest one-sixth and dimmest one-sixth of cells. Sorted cells were analyzed for clonogenic cell survival by incubating 600-2000 cells in tissue culture plates for 2 weeks before staining and counting colonies. A sample of 150,000 cells was also fixed in 70% ethanol and examined for γH2AX antibody binding.

Mouse Tumors: Growth and Treatment. SiHa xenograft tumors were grown s.c. in the flanks of non-obese diabetic/severe combined immunodeficient (NOD/SCID) mice as described previously (15). Mice bearing 0.4–0.6 *g* tumors were injected i.p. with etoposide or tirapazamine. At the same time, some mice received an injection of pimonidazole hydrochloride (100 mg/kg) that is metabolized and bound to hypoxic cells within the tumor (17). Ninety minutes later, mice were injected i.v. with 0.1 ml Hoechst 33342 (8 mg/ml stock) to label cells close to functional tumor blood vessels. Tumors were then excised, and a single cell suspension was prepared (17), and cells were sorted on the basis of Hoechst 33342 fluorescence using a Becton Dickinson FACS 440 cell sorter. Sorted cells were analyzed for clonogenic cell survival, and a sample of 150,000 cells was also fixed in 70% ethanol and examined for γH2AX antibody binding. Some experiments were also performed using 0.4–0.6 *g* SCCVII mouse squamous cell carcinoma cells transplanted s.c. in C3H/HeN mice. All of the experiments with mice were performed according to the guidelines of the Canadian Council on Animal Care.

Preparation of Spleen Cells. To prepare single cell suspensions from mouse spleen, minced tissue was incubated on a rotator at 37°C for 15 min in 5 ml PBS containing 1 mg/ml DNase, 0.4 mg/ml collagenase, and 2.5 mg/ml trypsin. Enzyme action was stopped by addition of MEM plus 10% fetal bovine serum followed by centrifugation and resuspension of the pellet in PBS. Cells were then fixed in 70% ethanol.

Flow Cytometry for γH2AX. Cells that were fixed in 70% ethanol were kept at −20°C for up to 2 weeks before analysis. Before antibody labeling, samples were rehydrated and incubated with mouse monoclonal anti-phospho-histone H2AX antibody (Upstate Biotechnology) as described previously (18). After 2 h at room temperature, cells were rinsed and incubated with 200 μl of secondary antibody [Alexa 488 goat-antimouse IgG (H + L)F(ab′)2 fragment conjugate; Molecular Probes] for 1 h at room temperature. Cells were rinsed and resuspended in 400 μl of cold Tris buffer containing 1 μg/ml ml 4′,6-diamidino-2-phenylindole (Sigma). Samples were analyzed for DNA content and γH2AX antibody binding using a Coulter Elite flow cytometer.

Image Cytometry for γH2AX in Sections. Frozen sections (5-μm thick) prepared from SiHa tumors and normal tissues were placed on slides, air-dried for no more than 1 min, and fixed in 2% freshly prepared paraformaldehyde for 15 min. Samples were then incubated for 30 min with anti-phospho-histone H2AX monoclonal antibody (Upstate Biotechnology) followed by rinsing and

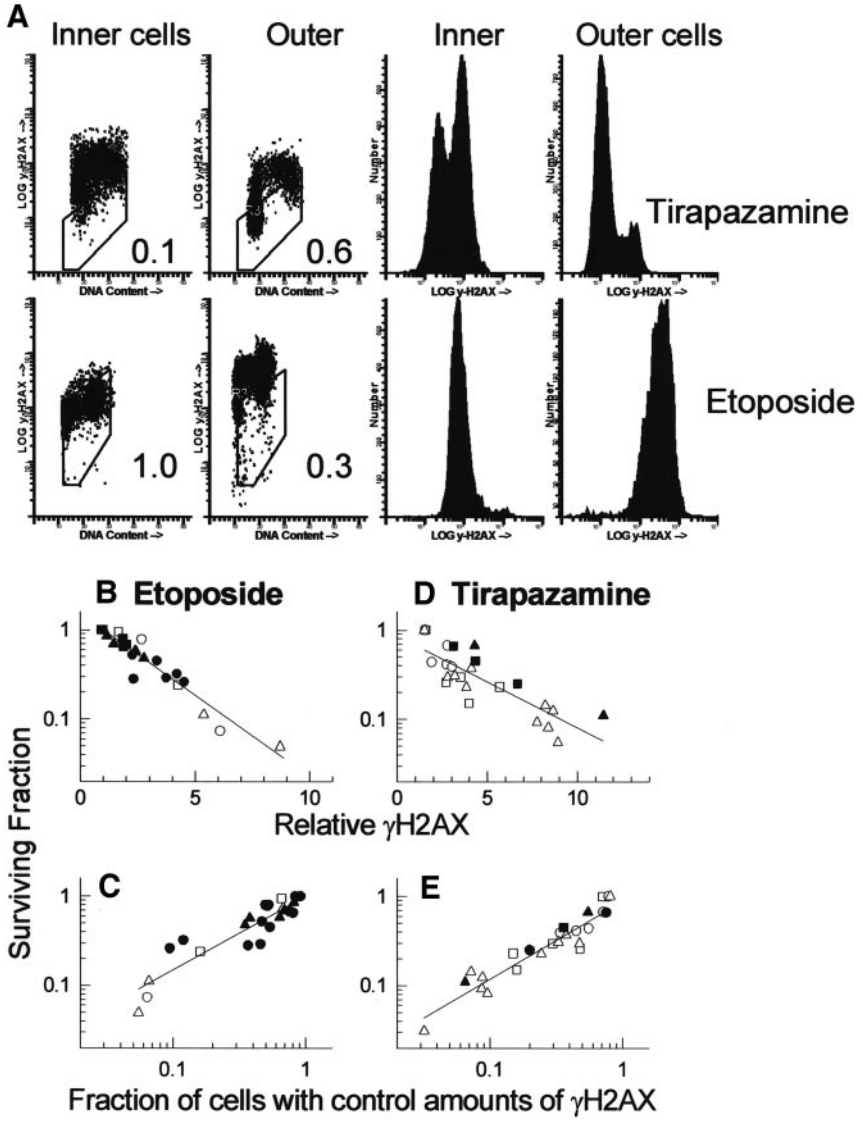

Fig. 1. Intensity of serine 139 phosphorylated histone H2AX (*γH2AX*) antibody staining in cells from spheroids. *A,* SiHa spheroids were exposed for 30 min to either 25 μg/ml 3-amino-1,2,4-benzotriazine-1,3-dioxide (*tirapazamine*) or 20 μg/ml etoposide, then incubated for 1 h to allow maximum γH2AX formation. Cells from trypsinized spheroids were then sorted to obtain inner and outer spheroid cells for analysis of γH2AX antibody binding and cell clonogenicity. The boxes encompass 95% of the cells from untreated spheroids, and the numbers next to the boxes indicate the fraction that fall within this range. These values were compared with clonogenic surviving fraction. *B–E,* SiHa spheroids (□, ○, and △) or V79 spheroids (■, ●, and ▲) were exposed to etoposide (10–50 μg/ml under ambient oxygen conditions) or to tirapazamine (11–55 μg/ml) under 10% oxygen gassing conditions. Cells were sorted from spheroids on the basis of the Hoechst 33342 diffusion gradient, and the symbols indicate whether cells came from the outer one-sixth (○, ●), inner one-sixth of spheroids (□, ■), or were unsorted (△, ▲). *B* and *D,* compare clonogenic surviving fraction with average γH2AX intensity relative to cells from untreated spheroids. *C* and *E,* compare clonogenic surviving fraction with the fraction of cells that show the same range of γH2AX intensities as untreated cells, as illustrated in Fig. 1. The best-fit line is shown for all of the data points.

incubation for 15 min with Alexa 488 goat antimouse IgG (Molecular Probes). Slides were dipped in paraformaldehyde, mounted with coverslips using 10 μl of Fluorogard (Bio-Rad), and sealed. Slides were viewed using a Zeiss Axioplan 2 fluorescence microscope, and images were acquired under constant light exposure conditions for each wavelength using a ×10 or ×100 Neofluor objective and a Q-Imaging 1350 EX digital camera. Images were captured and analyzed using Northern Eclipse and ImageJ software.

RESULTS

Exposure of multicell spheroids to etoposide and tirapazamine is known to produce cell killing and DNA damage that is dependent on the position of the cells within the spheroid. Damage by etoposide is confined largely to the external, proliferating cell layers of spheroids (19), whereas damage by tirapazamine occurs in the internal, hypoxic regions (20). Cell sorting based on the limited diffusion of the DNA binding dye Hoechst 33342 was used to obtain cells from the outer and inner layers of spheroids after a 30-min drug treatment and 1-h recovery. Some of these cells were examined for clonogenic potential, and the remainder was analyzed for γH2AX antibody binding. By analyzing cells at the peak time of γH2AX expression, cell cycle redistribution as a result of drug treatment was avoided, and the impact of DNA repair capacity was minimized. Fig. 1*A* shows typical γH2AX distribution profiles for the outer and inner cells from V79 spheroids exposed to etoposide or tirapazamine. The average levels of γH2AX antibody binding were increased for outer, proliferating cells exposed to etoposide relative to the innermost noncycling cells. The opposite pattern was seen for cells exposed to the bioreductive drug tirapazamine, where the innermost hypoxic cells preferentially metabolized the drug and showed a higher average γH2AX intensity. The fraction of cells that maintained background levels of γH2AX 1 h after a 30-min exposure to each drug is indicated by the boxed regions in the bivariate plots. Boxed regions take into account the greater expression of γH2AX in S/G_2-phase cells compared with G_1-phase cells (18), and they were matched to untreated cells analyzed at the same time using the same spheroid population. The fraction of cells within the box was consistent with the clonogenic fractions from the same treated populations measured in several independent experiments (Fig. 1*B*). Moreover, the relationship between γH2AX intensity and clonogenicity was the same for cells from spheroids prepared from V79 hamster lung fibroblasts and SiHa human cervical carcinoma cells (*open versus closed symbols*). Therefore, γH2AX antibody staining detected 1 h after a short treatment provides a rapid way to estimate cell sensitivity to killing by etoposide and tirapazamine that appears to be independent of cell type or microenvironment during treatment.

The time course of γH2AX development and loss after etoposide and tirapazamine treatment is shown in Fig. 2, *A* and *B*. SiHa spheroids were disaggregated at various times after treatment. A drug dose was chosen that killed the majority of the cells to minimize problems with repopulation during the recovery period, although the general pattern was confirmed using lower drug doses. Results confirmed a peak in expression occurring within 1 h after exposure to these drugs. There was a subsequent decline in γH2AX as a function of time after treatment with loss occurring more rapidly for etoposide-treated than tirapazamine-treated cells. It has been reported that the DNA-topoisomerase II complexes that form with tirapazamine are more stable than those that form with etoposide, and this may contribute to the longer retention of γH2AX (21). One hour after treatment, the fraction of cells that were clonogenic agreed well with the fraction of cells with control levels of γH2AX, designated by the cells falling within the boxes in the bivariate plots (Fig. 2*C*). By 24 h after treatment, there was an opportunity for both loss of foci and preferential loss of

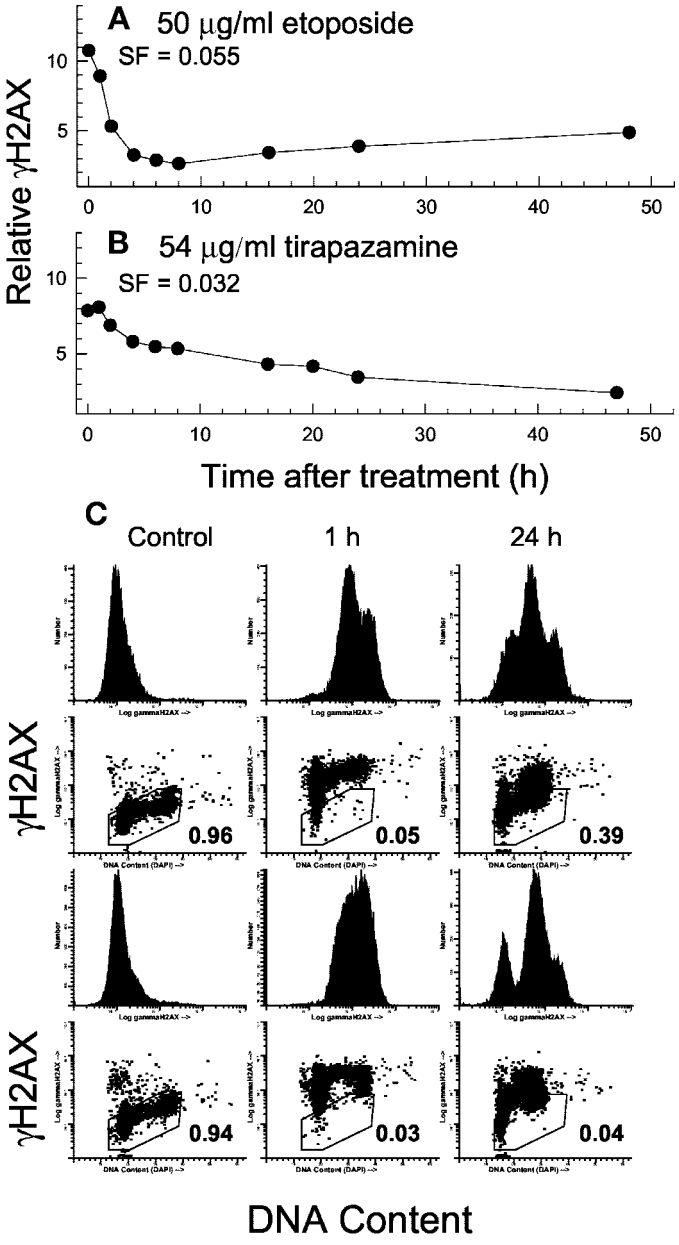

Fig. 2. Loss of serine 139 phosphorylated histone H2AX (*γH2AX*) after treatment of spheroids. *A* and *B*, kinetics of loss of γH2AX in SiHa spheroids exposed to etoposide or 3-amino-1,2,4-benzotriazine-1,3-dioxide (*tirapazamine*). The average amount of γH2AX/cell is shown relative to the untreated control cells for spheroids sampled at various times after a 30-min drug exposure. *C*, analysis of γH2AX expression in representative samples of SiHa spheroids after no treatment or at 1 or 24 h after a 30-min exposure to 50 μg/ml etoposide (*top 2 rows*) or 55 μg/ml tirapazamine (*bottom 2 rows*). The boxes indicate the gated regions containing the control cells and the fraction of the population that falls within these boxes.

damaged cells with foci. At this time, 41% of the cells of spheroids treated with tirapazamine exhibited control levels of γH2AX and 32% of the cells of these spheroids were clonogenic. This indicates that in addition to foci loss, loss of the more damaged cells had occurred. However, by 24 h after treatment with etoposide, 39% of cells showed normal levels of γH2AX, although the surviving fraction of this population was unchanged from 1 h after treatment. Therefore, the relationship between γH2AX expression and cell survival appears to be reliable for data obtained 1 h after exposure but not necessarily for samples analyzed 24 h after exposure.

To extend the spheroid results to a solid tumor model, immunodeficient mice bearing SiHa xenograft tumors were given a single i.p.

injection of 40 or 80 mg/kg etoposide followed 85 min later by an i.v. injection of Hoechst 33342 to label cells close to functional tumor blood vessels. The 90 min between drug injection and tumor excision was chosen to be consistent with the 30-min drug treatment of spheroids followed by a 1-h recovery period for foci formation. Tumors were excised 5 min later, and single cell suspensions were prepared. These cells were sorted on the basis of the Hoechst 33342 concentration gradient to obtain populations representing well-perfused and poorly perfused cells. As with spheroids, the fraction of cells that maintained background levels of γH2AX correlated with cell killing, regardless of position of the cells within the tumor cord (Fig. 3, *A* and *B*). Good correlations were obtained for both SiHa xenografts and SCCVII murine tumors. Therefore, γH2AX also appears to be a useful method for estimating tumor cell survival after exposure to etoposide *in situ*.

With tirapazamine, however, the fraction of cells with control levels of γH2AX was higher than the clonogenic survival in both SiHa and SCCVII tumor cells (Fig. 3, *C* and *D*). Because the expression of γH2AX is higher in S-phase than G_1- or G_2-phase monolayer cells after tirapazamine treatment (5), at least some foci may not develop until damaged cells, which are most likely to be hypoxic and nonproliferating, enter S phase. This would also explain the lower rate of loss of γH2AX in tirapazamine-treated compared with etoposide-treated spheroids (Fig. 3).

Frozen sections from SiHa xenografts were examined for the distribution of etoposide- and tirapazamine-induced γH2AX foci in relation to Hoechst 33342 and pimonidazole staining. Quantitative analysis of the relationship between Hoechst 33342 nuclear staining and γH2AX antibody binding was performed by first thresholding each image to identify "positive" pixels. We found that 30% ± 4% of the Hoechst-positive pixels were also positive for γH2AX after etoposide treatment, but only 10% ± 2% of the Hoechst-positive pixels were positive for γH2AX after tirapazamine treatment. To obtain information on relative intensity of staining through a tumor cord, profiles of γH2AX antibody and Hoechst 33342 fluorescence intensity were obtained from several tumor sections after etoposide or tirapazamine treatment. Representative images are

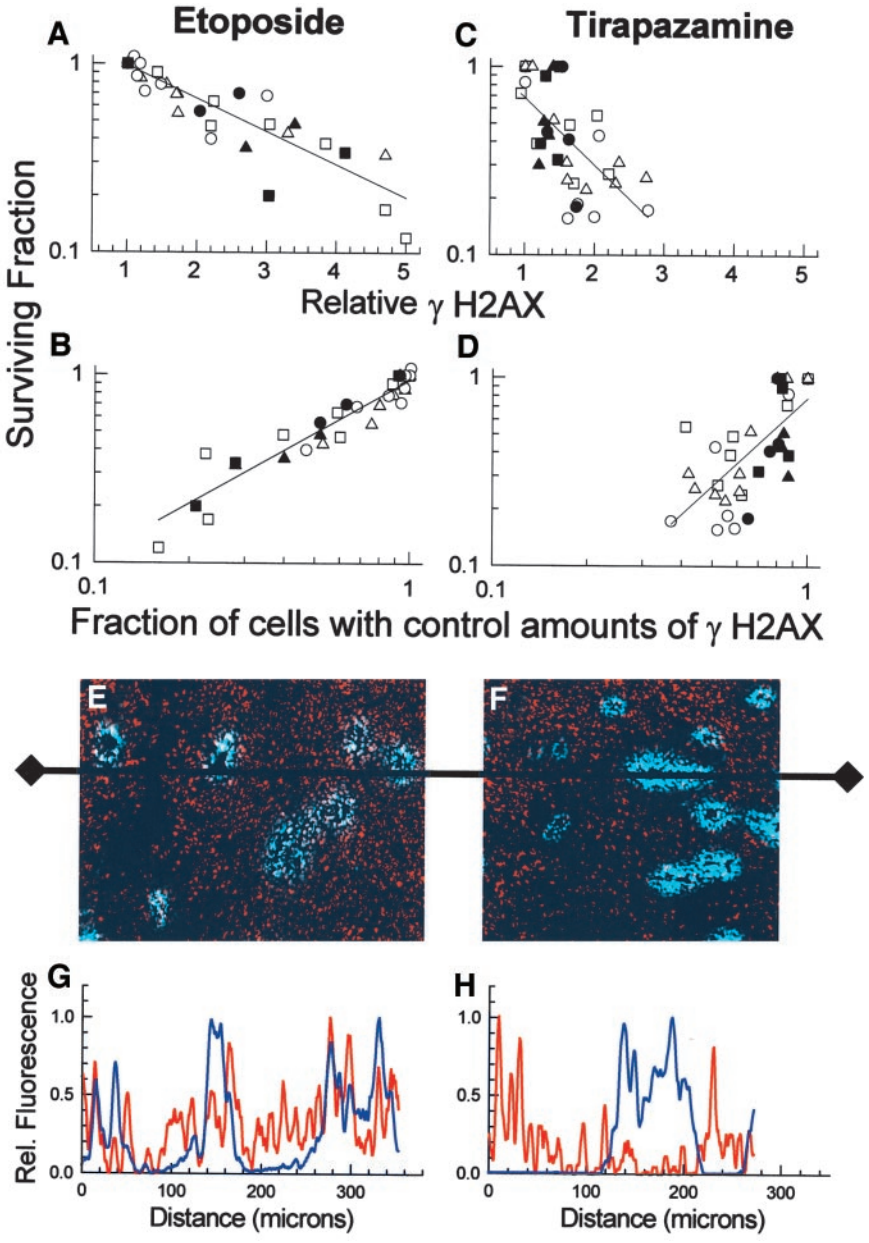

Fig. 3. Expression of serine 139 phosphorylated histone H2AX (*γH2AX*) after treatment of tumor-bearing mice with etoposide or 3-amino-1,2,4-benzotriazine-1,3-dioxide (*tirapazamine*). *A-3*, comparison between γH2AX expression and clonogenic surviving fraction in SiHa xenografts in immunodeficient mice (*open symbols*) and SCCVII tumors in C3H/H3J mice (*closed symbols*) exposed to etoposide (*A* and *B*) or tirapazamine (*C* and *D*). Tumor cells were recovered from mice 90 min after an i.p. injection of 40–80 mg/kg etoposide or 30–60 mg/kg tirapazamine and 5 min after an i.v. injection of Hoechst 33342. Cells were sorted on the basis of Hoechst 33342 concentration into fractions representing the poorly perfused cells (*circles*), well-perfused cells (*squares*), or unsorted populations of cells (*triangles*). The *top panel* shows the comparison between clonogenic survival and average amount of γH2AX antibody binding relative to cells from untreated mice. The *bottom panel* compares clonogenic surviving fraction with the fraction of cells that show the same range of γH2AX intensities as untreated cells. *E–H*, analysis of Hoechst 33342 and γH2AX in sections of SiHa xenografts exposed to 80 mg/kg etoposide (*E* and *G*) or 60/mg/kg tirapazamine (*F* and *H*). Frozen sections were prepared 90 min after drug injection and 5 min after Hoechst injection. Representative images are shown along with analysis of relative intensity of fluorescence across the indicated line; *blue* nuclei, Hoechst 33342 perfused; *red* nuclei, γH2AX antibody binding. Note that the well-perfused *blue-stained* cells show etoposide-induced DNA damage but not tirapazamine-induced damage.

Table 1 *Expression of γH2AX[a] in Hoechst 33342 stained cells*

Drug treatment	Relative amount of γH2AX in 20% dimmest Hoechst stained pixels[b]	Relative amount of γH2AX in 20% brightest Hoechst stained pixels	Ratio of γH2AX in perfused *versus* nonperfused regions
Etoposide	0.23 (0.003)[c]	0.62 (0.05)	2.6
Tirapazamine	0.35 (0.005)	0.14 (0.006)	0.4

[a] γH2AX, serine 139 phosphorylated histone H2AX; Tirapazamine, 3-amino-1,2,4-benzotriazine-1,3-dioxide.

[b] Images such as those shown in Fig. 3, *E* and *F*, were compared pixel by pixel. The maximum intensity of γH2AX and Hoechst 33342-positive pixels in each section was assigned the value of 1.0.

[c] Mean and SE for $n = 10–12$ sections.

shown in Fig. 3, *E* and *F*. Fig. 3, *G* and *H*, show the relative intensity of staining along a line drawn through two images. The maximum intensity of γH2AX and Hoechst 33342-positive pixels in each section was assigned the value of 1.0. Typically, cells labeled with γH2AX were found close to tumor blood vessels after etoposide treatment but distant from vessels after tirapazamine treatment. From these and similar images, γH2AX levels induced by etoposide were found to be 2.6 times higher in regions with the 20% highest levels Hoechst 333342 compared with the 20% lowest levels of Hoechst 33342 (Table 1). Conversely, tirapazamine-induced γH2AX levels were 2.5 times higher in the 20% of cells with the least Hoechst 33342 staining. This result was confirmed by examining γH2AX expression in regions of tumors that bound pimonidazole, a marker for hypoxic cells. Regions staining for pimonidazole showed low levels of γH2AX antibody staining after etoposide treatment. However, after tirapazamine treatment, pimonidazole-stained regions preferentially bound γH2AX antibodies (Fig. 4, *A–C*). Higher magnification confirmed the presence of nuclear foci (Fig. 4, *D–F*).

Because damage to normal tissues limits the dose of chemotherapeutic drugs that can be administered, selected normal tissues from control and drug-treated mice were also examined for γH2AX antibody staining. In mice exposed to tirapazamine or etoposide and sacrificed 90 min later, an increase in γH2AX staining was evident in some cells in frozen sections from kidney (Fig. 4, *G–I*). Similar results were obtained for thigh muscle (data not shown). Single cells prepared from mouse spleen were examined by flow cytometry. Responses were consistent with the presence of some spleen cells within the population expressing DNA damage after treatment of mice with etoposide and tirapazamine (Fig. 5, *A–F*). The percentage of cells falling within the control window was measured for spleen cells and tumors from the same mice, and the two values were plotted for each tumor type and drug (Fig. 5*G*). The relative amount of γH2AX measured 90 min after drug injection was similar for spleen cells and mouse tumors for both SiHa tumors growing in immunodeficient mice and SCCVII tumors in repair-proficient C3H/HeJ mice. Although immunodeficient mouse spleens are deficient in double-strand break repair, we were unable to detect any difference in response of the spleen cells from C3H and immunodeficient mice at this early time after exposure.

The ability to detect small populations of drug-resistant cells is limited by the difference in sensitivity between the two populations as well as by the number of cells that can be analyzed practically. We used previously the alkaline comet assay as a way to identify etoposide-resistant cells in mixtures with normal cells. Chinese hamster VP^r cells are ~5 times more resistant to DNA strand breakage and cell killing by etoposide than the parental V79 cell line (14), and we were able to resolve 1–2% resistant cells using the comet assay when 200 cells were analyzed (22). Because analysis of damage by flow cytometry allows rapid analysis of many more cells (150,000 were measured in these experiments), we expected the ability to resolve drug-resistant cells would increase. Results in Fig. 6 confirm the ability of γH2AX to resolve small subpopulations of resistant cells in known mixtures of etoposide-sensitive and resistant cells; however, resolution was not significantly improved relative to the comet assay as a result of the heterogeneity in γH2AX expression within each population.

DISCUSSION

The use of γH2AX to estimate clonogenic potential after treatment with etoposide and tirapazamine is based on the sensitive detection of an important lesion produced by these two drugs, the DNA double-strand break. In simple terms, cells lacking significant levels of γH2AX 1 h after exposure are likely to survive, whereas those cells

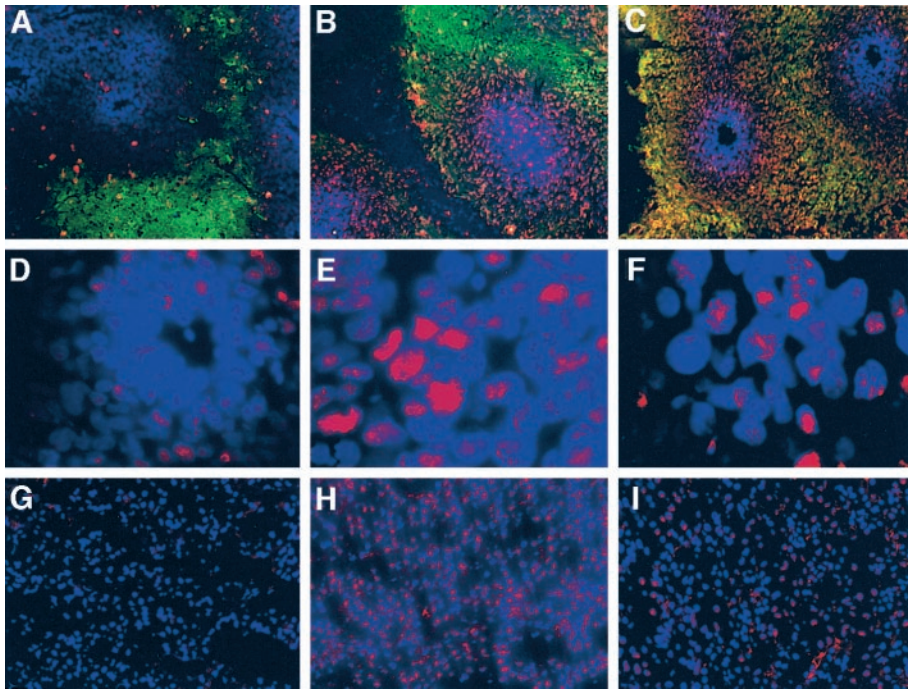

Fig. 4. Pattern of serine 139 phosphorylated histone H2AX (γH2AX) antibody staining in SiHa tumor sections and kidneys from mice exposed to etoposide or 3-amino-1,2,4-benzotriazine-1,3-dioxide (tirapazamine). Immediately after administration of the hypoxia marker pimonidazole, mice were injected with no drug (*A*), 80 mg/kg etoposide (*B*), or 60 mg/kg tirapazamine (*C*). Eighty minutes later, mice were given an i.v. injection of Hoechst 33342 that stains nuclei of perivascular cells blue. Tumors and kidneys were excised ~5 min later and frozen sections were prepared, fixed, and stained with antibodies against pimonidazole (*green*, cytoplasmic) and γH2AX (*red*, nuclear). Some brightly staining individual cells were seen in the control tumor (*A* and *D*) but no pattern was evident. Preferential staining of γH2AX after etoposide occurred in regions close to blood vessels that do not bind pimonidazole (*B* and *E*). Conversely, after tirapazamine, γH2AX levels were higher in regions distant from Hoechst-stained blood vessels that show pimonidazole antibody binding (*C* and *F*). Images in *A–C* are 275 microns wide. Images in *D–F* are taken at ×10 higher magnification to confirm the presence of drug-induced foci. Representative frozen sections kidneys of control (*G*), etoposide-treated (*H*) and tirapazamine treated mice (*I*) are also shown.

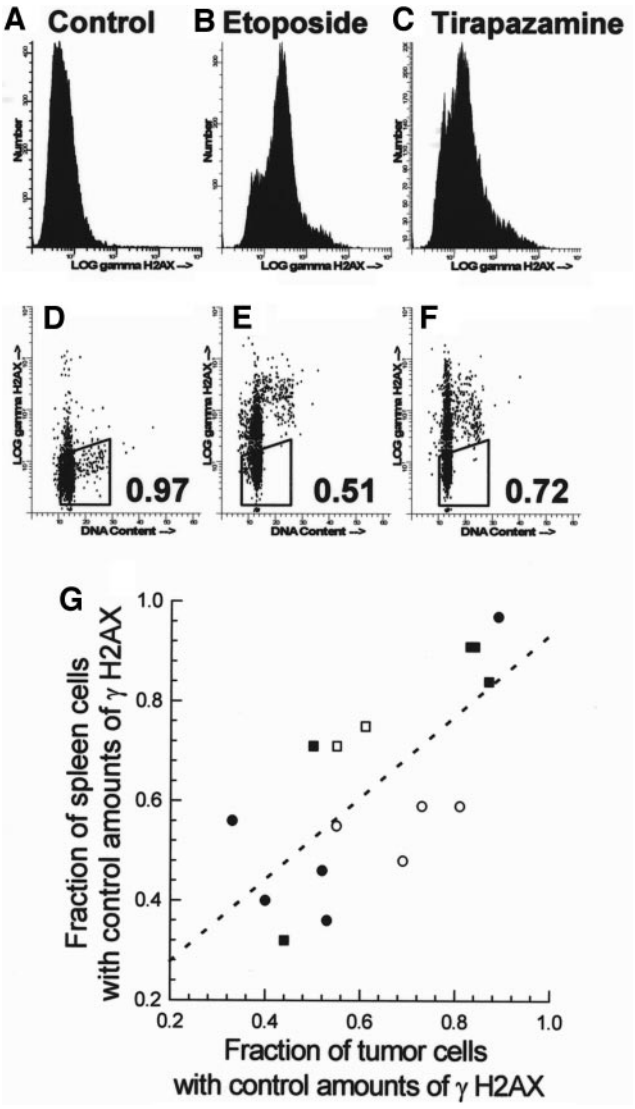

Fig. 5. Expression of serine 139 phosphorylated histone H2AX (*γH2AX*) in spleen cells from mice injected with 80 mg/kg etoposide or 60 mg/kg 3-amino-1,2,4-benzotriazine-1,3-dioxide (*tirapazamine*) and analyzed 90 min later. *A–C* show histograms of γH2AX antibody binding in mouse spleen cells analyzed using flow cytometry. Bivariate plots of DNA content *versus* log γH2AX antibody binding are shown beneath these histograms (*D–F*) together with the fraction of spleen cells that fall within the window. *E*, compares γH2AX expression in tumor and spleen cells from the same mouse exposed to various doses of etoposide (■, ●) or tirapazamine (○, □) for SiHa tumors (○, ●) or SCCVII tumors (■, □). Results are the average response of unsorted tumor cells.

with levels higher than the untreated cells are likely to die. This correlation was observed previously for exponentially growing V79 monolayers, and it is now shown to apply to V79 and SiHa cells grown as multicell spheroids (Fig. 1, *C* and *E*). Despite the significant increase in microenvironmental heterogeneity associated with this *in vitro* tumor model, the predictive ability of γH2AX was not compromised. These results suggest that the initial level of damage is the most important factor influencing tumor cell survival after treatment with these drugs.

When applying this method to the xenograft tumor model, etoposide continued to induce γH2AX levels that predicted cell death when measured 90 min after drug injection. After tirapazamine, however, only about half of the expected number of γH2AX-labeled cells was seen relative to the number of cells killed in the same population. Factors that could contribute to this change in response of tumors, but not spheroids, are long exposures to enzymes necessary for disaggregation of the tumors, lower plating efficiency of tumor cells, higher background levels of DNA damage, and different kinetics of "active removal" of dead cells. All but the latter of these factors should also influence results with etoposide, and one would need to invoke drug-specific death/disappearance mechanisms in tumors. There are two important differences between damage by tirapazamine and etoposide. Tirapazamine, but not etoposide, causes γH2AX foci to form preferentially in S-phase cells (5). This suggests that replication associated with sites of tirapazamine-induced damage may contribute to foci formation. Because hypoxic cells of tumors are very likely to be nonproliferating, damage by tirapazamine in these cells may be underestimated when γH2AX is measured 90 min after drug administration, which is before most cells attempt to synthesize DNA and proliferate. In spheroids, hypoxia was generated by equilibration with 10% oxygen; thus, many of the hypoxic cells in this model may have been proliferating. The second difference is that the cells most sensitive to tirapazamine are in a region of the tumor that is poorly supplied with nutrients; the kinase necessary for γH2AX formation may be less active. Preliminary support for this possibility is shown in Fig. 3, *C* and *D*; relative to the amount of cell kill, tumor cells close to blood vessels (*squares*) showed more damage than cells distant from blood vessels (*circles*).

The patterns of DNA damage by etoposide and tirapazamine were consistent with the preferential toxicity of etoposide toward proliferating cells and the preferential toxicity of tirapazamine for hypoxic cells. These patterns were evident in frozen sections of SiHa xenografts obtained after treatment with these drugs and with the hypoxia marker pimonidazole (Fig. 4, *A–C*). Quantitative imaging of individual tumor sections stained with the perfusion marker Hoechst 33342 and with γH2AX (both stains are nuclear) indicated that γH2AX expression after tirapazamine is ~2.5 times less likely to be associated with blood vessels than hypoxic regions distant from blood vessels. Conversely, γH2AX expression resulting from exposure to

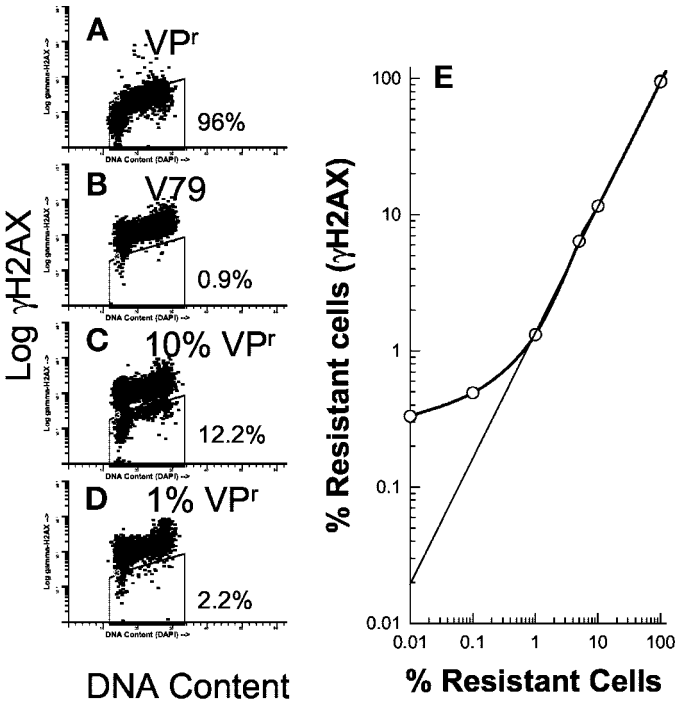

Fig. 6. Mixtures of etoposide-resistant Chinese hamster VP^r cells with etoposide-sensitive hamster V79 parental cells were prepared 1 h after a 30-min exposure to 10 μg/ml etoposide. Histograms show the serine 139 phosphorylated histone H2AX (*γH2AX*) antibody binding distributions relative to DNA content. *E*, shows the percentage of resistant cells based on the difference in γH2AX intensity.

etoposide was preferentially localized to regions surrounding vessels (Table 1). Antibody staining for γH2AX in relation to vascular areas may, therefore, be a useful way to determine the ability of DNA-damaging drugs to penetrate tumor tissue as well as the location of drug-resistant cells.

Few methods are available to rapidly estimate normal tissue response to cytotoxic treatment. For some agents, the expression of γH2AX may provide an indication of response of tumor *versus* normal cells *in situ*. The ability to measure DNA damage in a variety of normal tissues is possible using either flow cytometry for single cell suspensions or image analysis after staining tissues for γH2AX (Fig. 5). Samples of bone marrow cells or normal tissues recovered at the time of surgery would be potential sources of normal cells, providing cells could be obtained within an optimal time after drug treatment.

The peak expression of γH2AX occurred within 1 h after treatment with etoposide and tirapazamine, and the signal was lost with time after drug treatment. Fig. 2 indicated that there was retention of γH2AX in at least some cells at long times after drug treatment. It has been suggested that both rate of loss of γH2AX or residual foci may be useful indicators of cell sensitivity. Cells that retain even a few γH2AX foci at longer times after treatment may be more likely to die, however, resolving this small number from background or from replication associated γH2AX, especially in (tumor) cells that are genomically unstable, is likely to be difficult. Analysis at longer times can also be complicated by cell loss and production of apoptotic cells. Fig. 2*A* showed that 24 h after exposure of spheroids to etoposide, 39% of the cells showed background levels of γH2AX expression, although only 3% of cells were clonogenic. This result is similar to results observed previously for ionizing radiation, indicating that most γH2AX foci are lost from cells after lethal damage has been delivered, and, in fact, rate of loss was generally dose-independent (6). Therefore, the optimum time for γH2AX analysis is likely to be early after drug treatment. Whether γH2AX expression will be sufficiently sensitive for detection of damage using clinical schedules will need to be determined for each drug and drug combination.

REFERENCES

1. Kurbacher CM, Grecu OM, Stier U, et al. ATP chemosensitivity testing in ovarian and breast cancer: early clinical trials. Recent Results Cancer Res 2003;161:221–30.
2. Olive PL, Banáth JP. Multicell spheroid response to drugs predicted with the comet assay. Cancer Res 1997;57:5528–33.
3. Olive PL, Johnston PJ, Banáth JP, Durand RE. The comet assay: a new method to examine heterogeneity associated with solid tumors. Nat Med 1998;4:103–5.
4. Olive PL, Vikse CM, Banáth JP. Use of the comet assay to identify cells sensitive to tirapazamine in multicell spheroids and tumors in mice. Cancer Res 1996;56:4460–3.
5. Banath JP, Olive PL. Expression of phosphorylated histone H2AX as a surrogate of cell killing by drugs that create DNA double-strand breaks. Cancer Res 2003;63:4347–50.
6. MacPhail SH, Banath JP, Yu TY, et al. Expression of phosphorylated histone H2AX in cultured cell lines following exposure to X-rays. Int J Radiat Biol 2003;79:351–8.
7. Rogakou EP, Boon C, Redon C, Bonner WM. Megabase chromatin domains involved in DNA double-strand breaks in vivo. J Cell Biol 1999;146:905–16.
8. Andegeko Y, Moyal L, Mittelman L, et al. Nuclear retention of ATM at sites of DNA double strand breaks. J Biol Chem 2001;276:38224–30.
9. Limoli CL, Giedzinski E, Bonner WM, Cleaver JE. UV-induced replication arrest in the xeroderma pigmentosum variant leads to DNA double-strand breaks, gamma-H2AX formation, and Mre11 relocalization. Proc Natl Acad Sci USA 2002;99:233–8.
10. Huang X, Traganos F, Darzynkiewicz Z. DNA damage induced by DNA topoisomerase I- and topoisomerase II-inhibitors detected by histone H2AX phosphorylation in relation to the cell cycle phase and apoptosis. Cell Cycle 2003;2:614–9.
11. Liu JS, Kuo SR, Beerman TA, Melendy T. Induction of DNA damage responses by adozelesin is S phase-specific and dependent on active replication forks. Mol Cancer Ther 2003;2:41–7.
12. Rothkamm K, Lobrich M. Evidence for a lack of DNA double-strand break repair in human cells exposed to very low x-ray doses. Proc Natl Acad Sci USA 2003;100:5057–62.
13. Bonner WM. Low-dose radiation: thresholds, bystander effects, and adaptive responses. Proc Natl Acad Sci USA 2003;100:4973–5.
14. Luo C, Johnston PJ, MacPhail S, et al. Cell fusion studies to examine the mechanism for etoposide resistance in Chinese hamster V79 spheroids. Exp Cell Res 1998;243:282–9.
15. Olive PL, Banath JP, Durand RE. The range of oxygenation in SiHa tumor xenografts. Radiat Res 2002;158:159–66.
16. Durand RE, Olive PL. Resistance of tumor cells to chemo- and radiotherapy modulated by the three-dimensional architecture of solid tumors and spheroids. Methods Cell Biol 2001;64:211–33.
17. Olive PL, Durand RE, Raleigh JA, Luo C, Aquino-Parsons C. Comparison between the comet assay and pimonidazole binding for measuring tumour hypoxia. Br J Cancer 2000;83:1525–31.
18. MacPhail SH, Banath JP, Yu Y, Chu E, Olive PL. Cell cycle-dependent expression of phosphorylated histone H2AX: reduced expression in unirradiated but not x-irradiated G(1)-phase cells. Radiat Res 2003;159:759–67.
19. Olive PL, Banath JP, Evans HH. Cell killing and DNA damage by etoposide in Chinese hamster V79 monolayers and spheroids: influence of growth kinetics, growth environment and DNA packaging. Br J Cancer 1993;67:522–30.
20. Olive PL. Detection of hypoxia by measurement of DNA damage in individual cells from spheroids and murine tumours exposed to bioreductive drugs. I. Tirapazamine Br J Cancer 1995;71:529–36.
21. Peters KB, Brown JM. Tirapazamine: a hypoxia-activated topoisomerase II poison. Cancer Res 2002;62:5248–53.
22. Huang P, Olive PL, Durand RE. Use of the comet assay for assessment of drug resistance and its modulation in vivo. Br J Cancer 1998;77:412–6.